Quasifree Scattering of 160-MeV Protons from Nuclei*

N. S. WALL AND P. R. Roos†
Massachusetts Institute of Technology, Cambridge, Massachusetts and University of Maryland, College Park, Maryland‡
(Received 9 June 1966)

Using 160-MeV protons and a NaI total-energy scintillation counter we have measured the spectra of outgoing protons from 40 to 160 MeV at angles of 10–80 deg for a number of targets, Be^9, C^{12}, Ca^{40}, Ni^{58}, Sn^{120}, and Bi^{209}. The data have been interpreted by means of an impulse-approximation calculation. We have modified the usual analysis to calculate the scattering from nuclei, for which we assume that an extreme shell model is a valid representation. The differential cross section thus calculated can be expressed in terms of the momentum of the struck nucleon. We find that the shell-model description does not give enough high-momentum components to the nucleon wave functions. This is deduced because the experimental results necessitate high-momentum components to be able to produce high-energy large-angle outgoing protons.

I. INTRODUCTION

IN high-energy proton-nucleus scattering experiments ($E \geq 100$ MeV), one usually invokes the impulse approximation[1] to interpret the experimental results.[2] In the impulse approximation one considers the incoming proton as interacting with individual nucleons in the nucleus, and replaces this interaction by the free nucleon-nucleon interaction, neglecting off-the-energy-shell effects. Using the simple impulse approximation (the incident particle only interacts through a nucleon-nucleon interaction, once with the target nucleus), we would expect at a given angle the following proton energy spectrum in a single detector experiment[3] for an incident energy below π-meson threshold:

Starting at the highest energy, we would expect a peak corresponding to elastic scattering. In the next approximately 20 MeV we would expect a series of peaks, corresponding to inelastic scattering to discrete states, though the detailed spectrum would depend critically upon the over-all energy resolution. This inelastic scattering corresponds to a coherent interaction between the incident proton and those target nucleons in the configurations which make up the excited state.[4] Finally, one expects a very broad peak, with the maximum at an energy approximately the same as though the incident nucleon were scattered through the same angle by a free nucleon.

This type of analysis has also been discussed in detail by Fowler and Watson[5]; however, their definitions of the term "quasi-elastic" refers to what we have called the inelastic scattering to discrete states. The process commonly referred to as "quasi-elastic" or "quasifree" scattering is their "direct inelastic" scattering.

The width of this so-called quasi-elastic peak should reflect the internal momentum of the nucleons in the nucleus, and a measurement of this spectrum may give us information on the nucleon momentum distribution, insofar as the impulse approximation is valid and we are observing a single scattering. If one includes multiple scattering, as we must, since we know the free nucleon-nucleon cross sections to be large, there will be a general filling in of the low-energy region owing to particles undergoing more than one collision and therefore losing more energy. The large nucleon-nucleon cross section also accounts for the large imaginary component of the optical potential[1] so that all absorptive processes might be expected to modify the spectrum. These points are discussed in more detail in Secs. III and IV.

In this experiment we studied the quasifree scattering region of the spectrum. Similar experiments have been performed at 320 MeV[6] and 660 MeV[7] and indeed, one does see the structure described above. Experiments have also been performed with electrons on C^{12} (Ref. 8) and Bi^{209} (Ref. 9) yielding similar results. The experiments reported here utilize an energy resolution much better than that used in the previous experiments, and therefore significantly smaller than the width of the peak. Furthermore, the lower energy of this experiment affords an opportunity to gauge the effects of multiple scattering. Such effects are so severe

* That part of the work at Massachusetts Institute of Technology was supported by the U. S. Atomic Energy Commission under Contract AT(30-1)-2098. That portion of the work at the University of Maryland was supported by grants from the Research Board of the University of Maryland and by the U. S. Atomic Energy Commission under Contract AT(40-1)-3491.

† Now at Oak Ridge National Laboratory. This work was, in part, a section of the Ph.D. thesis submitted to MIT.

‡ The various calculations referred to herein were done both at the MIT Computer Science Center and the University of Maryland Computer Science Center. The calculations at the University of Maryland were supported under National Aeronautics and Space Administration Grant No. NSG 398.

[1] A. K. Kerman, H. McManus, and R. M. Thaler, Ann. Phys. (N. Y.) 8, 551 (1959).

[2] A. B. Clegg, *High Energy Nuclear Reactions* (Oxford University Press, London, 1955); G. Jacob and T. Maris, Rev. Mod. Phys. 38, 121 (1966).

[3] K. W. McVoy and L. VanHove, Phys. Rev. 125, 1034 (1962).

[4] R. Haybron and H. McManus, Phys. Rev. 140, B638 (1965).

[5] T. K. Fowler and K. M. Watson, Nucl. Phys. 13, 549 (1959).

[6] J. B. Cladis, W. N. Hess, and B. J. Moyer, Phys. Rev. 87, 425 (1952).

[7] L. S. Azhgirey *et al.*, Nucl. Phys. 13, 258 (1959).

[8] J. E. Leiss and R. E. Taylor (private communication) and see Ref. 24.

[9] H. Kendall and B. Isabelle (private communication).

at 96 MeV that Strauch and Titus[10] barely, if at all, see a quasi-elastic peak at 45°, whereas at the higher energies such a peak is apparent.

With respect to the analysis we present in Sec. IV, while following the essential idea of Wolff,[11] it is more detailed than that of Refs. 6, 7, and 11. Calculations for quasi-elastic scattering for the 320-MeV data on C^{12} and O^{16} at 30° and 40° were done by Wolff.[11] Azghirey *et al.*[7] used the same general description in the analysis of their experiments at 660 MeV. These calculations will be described more fully later, but they are based on the impulse approximation of Chew and Wick[12,13] in which case one obtains

$$\frac{d^2\sigma}{d\Omega dE}\sim\left(\frac{d\sigma}{d\Omega}\right)_{p,\text{nucleon}}\sum_{i=1}^{A}\int|\Psi_i(\mathbf{q})|^2 d\mathbf{q}, \qquad (1)$$

where $(d\sigma/d\Omega)_{p,\text{nucleon}}$ is the free proton-nucleon scattering cross section, and $\Psi_i(\mathbf{q})$ is the Fourier transform of a single-particle wave function. In Wolff's calculations he assumed that the average nuclear momentum distribution was a Gaussian or some other simple analytic expression defined by one parameter, a characteristic momentum of a nucleon in a nucleus. This means that the sum in Eq. (1) reduces to A times one integral. Similar calculations were made by Azghirey *et al.*, including relativistic kinematics and using the sum of two Gaussian distributions to represent the momentum distribution. Their calculations gave similar results for the momentum distributions. A different approach to the analysis of such experiments has been followed by Bertini[14] using Monte Carlo techniques. This calculation includes the multiple scattering of the particles in the nucleus. A further discussion of the method and the results of these calculations will be given in Sec. 4.

In both of these approaches a simple impulse approximation is assumed to be valid. Trammel and Chalk[15] recently gave as a criterion for the neglect of multiple-collision processes that the quantity $\rho=(\xi/R)\times(v_2/v_1)^3$ be small. In this expression ξ is the scattering amplitude, R a measure of the size of the scatterer, v_1 the speed of the outgoing particle, and v_2 the speed of the struck particle in its initial state. We estimate ρ to be of order 0.1, which while not too small, leads one to expect strong single-collision phenomena down to outgoing proton energies of the order of $\frac{1}{2}$–$\frac{1}{4}$ of the incident energy in these experiments. Even if multiple-scattering effects can be neglected, it has been pointed out by Gottfried[16] that at high momentum transfer (large compared to the Fermi momentum) the validity of the simple impulse approximation is open to question. It is to be hoped that the deviations of our experiment from a simple, individual-particle impulse-approximation prediction (with no account taken of the detailed trajectories of the incident and observed particle through an optical potential) can point out nuclear correlations or deviations from the impulse approximation.

II. EXPERIMENT

We have measured the energy distribution of protons produced in the interaction of 160-MeV protons with nuclei detecting only a single proton. The energy distribution has been measured from 40 to 160 MeV in 10° steps from 20° to 80°. The targets used were Be^9, C^{12}, Ca^{40}, Ni^{58}, Sn^{120}, and Bi^{209}.

The experimental arrangement has been described previously.[17] It essentially consisted of a counter telescope mounted on a 5-ft arm which could be rotated about the target to ~85°. The target was placed in a small scattering chamber (~13 in. in diameter) to reduce scattering of the incident beam by air into the counter. The counter telescope consisted of two thin plastic scintillators (~0.5 g/cm²) and a 3-in.×3-in. NaI Harshaw integral line-selected scintillation counter to measure the proton energy. A coincidence was required between the two plastic scintillators and this coincidence gated a multichannel analyzer which stored the NaI pulse. The resolution of the NaI crystal was $\frac{3}{4}\%$ for 160-MeV protons. Since in this experiment we also wished to measure elastic scattering, it was necessary to make the sum of the two plastic scintillators 1 g/cm² (~5 MeV for 160-MeV protons) in order to stop the elastically scattered protons in the NaI crystal. This and the NaI housing places approximately a 35-MeV lower limit on the proton energy.

The use of NaI or for that matter any scintillation counter at high energies does have one disadvantage. Some of the protons entering the crystal will undergo nuclear interactions in the crystal, giving rise to a substandard pulse height. Thus for every peak in the spectrum there corresponds a tail which extends over the full energy range. In fact, at 160 MeV the tail-to-peak area ratio is approximately 25%.[17,18] Measurements of the tail-to-peak ratio for NaI have been made from 0 to 40 MeV[19] and 50 to 160 MeV.[18] These measurements show that the tail-to-peak ratio roughly follows and E^2 dependence. Also, the tail associated with the peak appears to be rather flat over the entire range. In order to correct the data for this effect, a program was written which made corrections to the spectrum using an E^2 dependence for the tail-to-peak ratio, and assuming a flat tail. An iterative process was used

[10] K. Strauch and Titus, Phys. Rev. **104**, 191 (1956).
[11] P. A. Wolff, Phys. Rev. **87**, 434 (1952).
[12] G. F. Chew and G. C. Wick, Phys. Rev. **85**, 636 (1952).
[13] G. F. Chew and M. L. Goldberger, Phys. Rev. **87**, 778 (1952).
[14] H. Bertini (private communication) and Phys. Rev. **131**, 1801 (1963).
[15] G. T. Trammel and J. D. Chalk, Phys. Rev. **141**, 815 (1966).
[16] K. Gottfried, Ann. Phys. (N. Y) **21**, 29 (1963).
[17] P. G. Roos and N. S. Wall, Phys. Rev. **140**, B1237 (1965). See also P. G. Roos, Ph.D. thesis, MIT, 1964 (unpublished).
[18] D. Measday, Nucl. Instr. Methods **34**, 353 (1965).
[19] L. H. Johnston, D. H. Service, and D. A. Swenson, IRE Trans. Nucl. Sci. **NS-5**, 95 (1958).

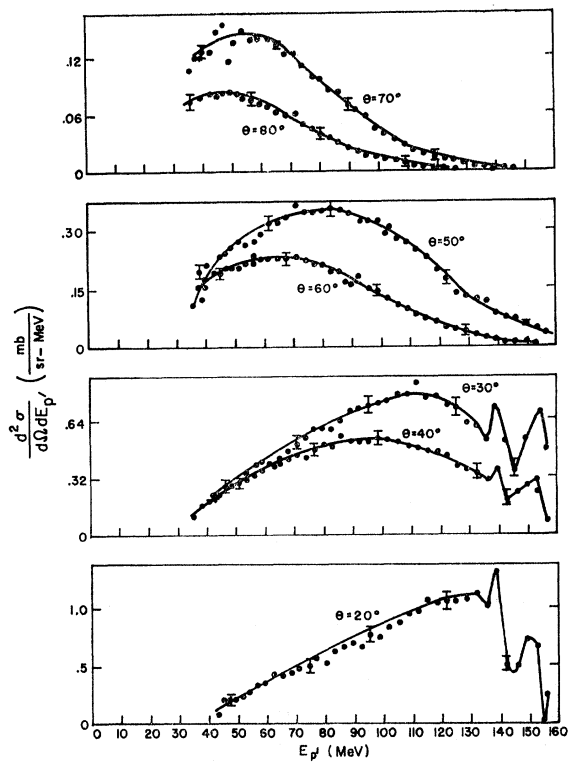

FIG. 1. The differential cross section for the reaction $C^{12}(p,p')$ as a function of the energy of the outgoing protons for the angles indicated. In this and subsequent spectra the peak arising from elastically scattered protons has been suppressed and we have averaged over an energy integral such that low-lying discrete states are not clearly seen. The data have not been corrected for the scattering out caused by the plastic scintillators. This makes a negligible change in the shape of the spectra, except at angles of 60° and larger where the broad peak in the spectrum is washed out.

which started at the high-energy end of the spectrum and proceeded to the low-energy end. The corrected spectrum did not differ greatly from the raw spectrum, though there was a slight shift of the quasi-elastic peak to higher energy.

The absolute cross sections were obtained by normalizing the inelastic scattering to the 4.43-MeV state in C^{12} to the data taken at Orsay[20] and Harwell.[21] The error bars are mainly statistical, though estimates of the error in the use of a flat reaction tail have been inculded. Typical error bars are shown in Fig. 1. The data shown in Fig. 1 have not been corrected for scattering-out by the first scintillation counter (the second causes a completely negligible loss). The data in subsequent figures have been corrected using a set of programs developed by Ball.[22] The magnitude of the correction is about 30% at 40 MeV, dropping sharply to 13% at 50 MeV, and is well within statistical error by 90 MeV, where it introduces a 1% correction.

[20] J. P. Garron *et al.*, J. Phys. Radium **21**, 317 (1960).
[21] D. J. Rowe *et al.*, Nucl. Phys. **54**, 193 (1964).
[22] J. B. Ball (private communication) Oak Ridge National Laboratory Report No. ORNL 3311 (unpublished).

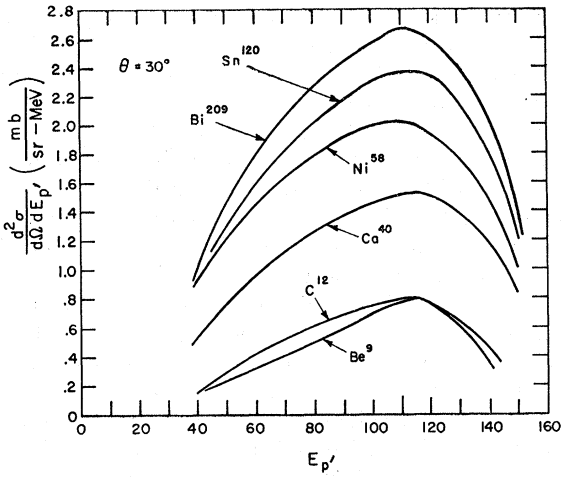

FIG. 2. The differential cross section for the elements indicated as a function of the outgoing proton energy at a laboratory angle of 30°.

In addition one run was made with particle identification using the plastic scintillators as dE/dx counters, in order to estimate contamination of the spectrum from particles other than protons. It was found that deuterons make up 5–10% of the spectra, and other particles gave negligible contributions.

III. RESULTS

The results for the full proton energy spectrum (40 to 160 MeV) are shown for C^{12} in Fig. 1. In these data we observe a very broad peak (~80 MeV) with a maximum that shifts to lower energy with increasing angle. The data for the other targets are all very similar to those of carbon, as is shown in Figs. 2 and 3 for 30°

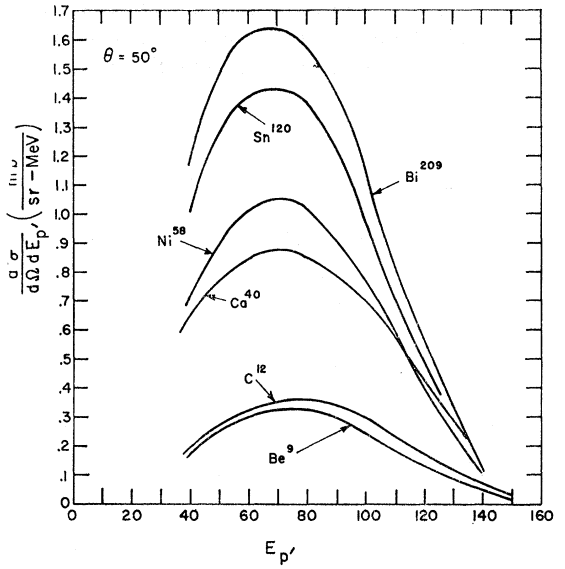

FIG. 3. The differential cross section for the elements indicated as a function of the outgoing proton energy at a laboratory angle of 50°.

and 50°, respectively. In these figures the data have been plotted for all nuclei at a given angle. In Figs. 2 and 3 we see that, in general, the peak maxima and shapes are the same for all nuclei and that the cross section increases with increasing A.

To get a better idea of the similarities between different nuclei, we have normalized all the data to Bi^{209} (Figs. 4 and 5). In these figures we can see even more clearly the remarkable similarity among all of the nuclei. One would expect such similarity in the shapes and positions of the peaks on the basis of the simple impulse approximation (single scattering) and the shell model, which predicts a similar momentum distribution and average binding energy for all nuclei. If, however, there are large contributions due to multiple scattering in the nucleus, one expects a general filling in on the low-energy side of the peak, provided small energy losses are not allowed. Such inhibition is to be expected on the basis of the Pauli principle and the shell model. If the multiple-scattering contribution in these experiments were large, the low-energy side of the peak for Bi^{209} should look significantly different from that for Be^9. This is not the case in these data, and we are led to suspect that either the multiple scattering is small, or that, if more than one scattering take splace, there is sufficient energy loss to bring the proton below our threshold, so that in effect we are observing primarily single scattering. Our spectra also suggest that even though multiple-proton emission is energetically possible following the first scattering, if such processes occur, the energy of the secondary outgoing protons would be below our threshold. That the secondary protons might now have energy can be seen because first of all to a high degree of accuracy (see Sec. IV), the incident particle ejects a particle from a shell-model state which would lead to fairly low excitation energies of the residual nucleus because the important shell-model states are only slightly bound. Secondly, even if

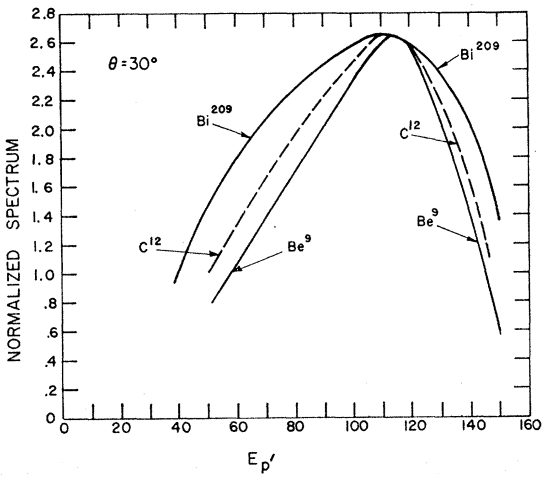

FIG. 4. The data of Fig. 2 normalized to Bi^{209} to enable the differences between various nuclei to be accentuated.

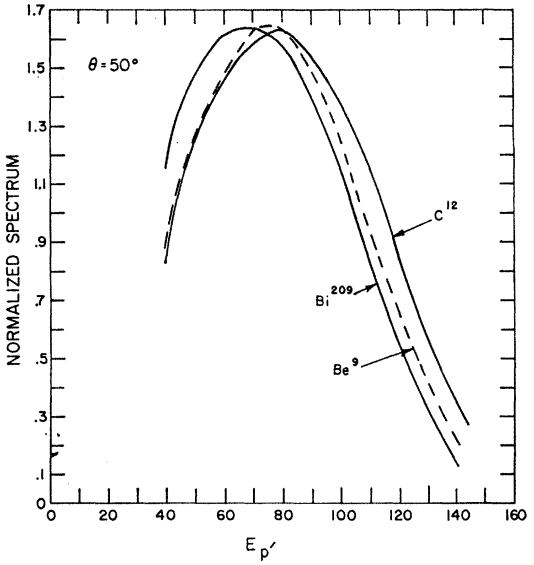

FIG. 5. The data of Fig. 3 normalized to Bi^{209} to enable the differences between various nuclei to be accentuated.

the excitation energy of the residual nucleus were relatively high ($\sim E_{\text{inc}}/2$) the secondary proton might still undergo sufficient subsequent scattering to fall below our experimental threshold.

Thus far, we have been assuming that the broad peak in the proton continuum is due to quasi-elastic scattering by individual target nucleons. One can get an idea of the validity of this assumption by several methods. First, we have plotted the peak maximum energy versus angle for the data in Fig. 6. Also included in this plot is the free nucleon-nucleon kinematics curve. The error bars on the experimental points are such that include the peak maxima for all nuclei. We see that there is quite good agreement between the data and the free nucleon-nucleon kinematics, thus supporting our belief that the peak is the result of quasi-elastic scattering. The data, however, do have a smaller slope than the nucleon-nucleon kinematics. This can be explained fairly well at small angles by taking into account the fact that the nucleons are bound as will be shown in Sec. IV.

If the scattering process were as simple as we described, and there were no absorption phenomena to contend with, the cross section would be proportional to A. In Fig. 7 the ratio of σ_{total} (40 to 160 MeV) to $(N\sigma_{p,n}+2Z\sigma_{p,p})$ has been plotted as a function of A. The quantity σ_{total} (40–160 MeV) is the total cross section for protons with energies between 40 and 160 MeV measured in this experiment, and $\sigma_{p,n}$ and $\sigma_{p,p}$ are the free proton-neutron and proton-proton reaction cross sections, about 48 and 24 mb, respectively. From this plot we see that not all of the nucleons enter into the reaction, since if they did and single-nucleon scattering were the dominant process this ratio would be unity. In other words, the shape of this curve allows

us to obtain an indication of the relative absorption between different nuclei, and shows that a smaller percentage of nucleons enter the reaction as A increases.

Table I gives the observed cross sections[23] integrated on energy and angle assuming a constant differential cross section for angles beyond those measured. These cross sections are compared with the total reaction cross section, and it is seen that even for the heaviest nuclei the events we believe to be single scattering make up more than one-third of the total cross section. There is no problem arising in light nuclei because the process we are looking at represents a large fraction of the total cross section. We only detect one particle coming out and say nothing about any other particle.

IV. CALCULATION

To interpret our data, we have extended the calculations of Wolff in Ref. 11.[24,25] The basic calculation he did was to evaluate, within the framework of the impulse approximation with no multiple scattering, the differential cross section for scattering an incident particle from a collection of A nucleons with a given momentum distribution. Our calculation differs in two essential respects from his. First of all, we do not assume an over-all momentum distribution, but, in fact, derive a momentum distribution for each single particle state in the nucleus. Secondly, we have taken the binding energy, B_{if} in Wolff's notation, as the single particle separation energy as measured in a $(p,2p)$ or pickup experiment[2] In this approximation the expression derived by Wolff takes on the form

$$\frac{d^2\sigma}{d\Omega dE}=2\frac{M}{\hbar^2}\frac{q}{p|\mathbf{p}-\mathbf{q}|}\sum_i N_i\int_{K_{\min}}^{\infty}|\psi_i(k)|^2\frac{d\sigma_i}{d\Omega}(\theta)kdk, \quad (2)$$

where $d^2\sigma/d\Omega dE$ is the cross section for scattering a proton of initial momentum $\hbar p$ and final momentum $\hbar q$ (energy E) by a nucleon in the nucleus of momentum $\hbar k$. M is the nucleon mass, $|\Psi_i(k)|^2$ is the square of the normalized Fourier transform of the ith particle nucleon state, N_i is the number of such nucleons, and $d\sigma_i/d\Omega(\theta)$ is the nucleon-nucleon center-of-mass differential cross section for the scattering by an ith nucleon. $K_{\min}$ is that minimum momentum which a nucleon must have to be observed at a scattering angle θ, with an energy E if it has a binding energy in the nucleus B_{if}. $K_{\min}$ is defined by Eq. (8) of Ref. 11, and in evaluating it we have made no approximations. In the analysis we have made, we have treated the nucleon-nucleon differential cross as a constant equal to approximately (within 10% over most of the angular range) the p-p cross section at 160 MeV, specifically 3.53 mb/sr.[26-28]

To derive the single-particle states which were Fourier eransformed to give $|\Psi_i(k)|^2$, we utilized the ABACUS II program of Auerbach.[29] For Ca^{40}, following Elton *et al.*[30] (who find single-particle energy-dependent potentials that give rise to a change-density distribution which fits the electron-scattering data), we chose a Saxon-shaped shell-model potential with parameters whose values are those shown in Table II. For Be^9 we were not able to find a single shell-model potential which fit both the $1p_{3/2}$ binding energy of 17.5 MeV and $1s_{1/2}$ value of 27 MeV. We instead searched on the

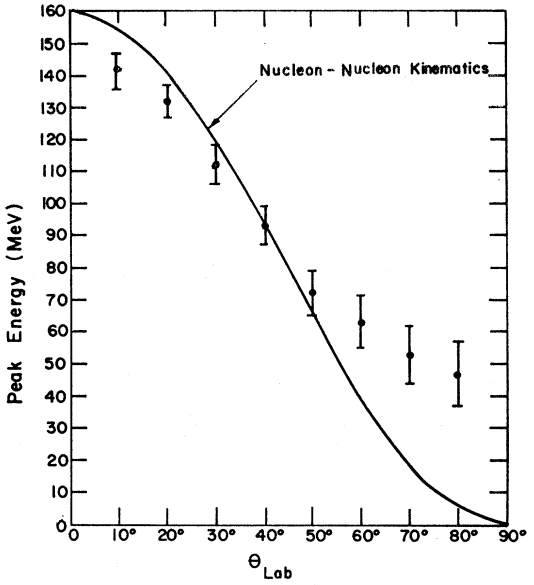

FIG. 6. The energy of the outgoing protons at the peak of the quasifree scattering spectrum as a function of the scattering angle. The error bars represent the span of the peak energy for the various targets. The free nucleon-nucleon kinematics curve shown is nonrelativistic, but a relativistic one is only very slightly different. At angles greater than 60°, our estimate of the peak position is rather poor because the scattering out by the plastic scintillators distorts the spectrum appreciably.

TABLE I. The total quasi-free scattering cross section σ_{qf} for the various targets studied, and the ratio of that cross section to the total nuclear reaction cross section, σ_t.

Target	Total quasifree cross section	Total reaction cross section[a]	σ_{qf}/σ_t
Be^9	159±11	186	0.84
C^{12}	187±13	212	0.88
Ca^{40}	407±29	524	0.78
Ni^{58}	523±37	662	0.79
Sn^{120}	649±45	1165	0.56
Bi^{209}	715±50	1790	0.40

[a] See Ref. 23.

[23] A. Johansson, V. Svanberg, and O. Sandberg, Arkiv Fysik **19**, 572 (1961).

[24] A calculation similar to ours, but for inelastic electron scattering, was done by Czyż in the analysis of the unpublished experiments of Leiss and Taylor. The experimental results are in Ref. 25.

[25] W. Czyż, Phys. Rev. **131**, 2141 (1963).

[26] K. F. Riley, Nucl. Phys. **13**, 407 (1959).

[27] R. Wilson, *Nuclear-Nucleon Scattering, Experimental Aspects* (Interscience Publishers, Inc., New York, 1963).

[28] M. J. Moravcsik, *The Two-Nucleon Interaction* (Oxford University Press, London, 1963).

[29] E. H. Auerbach (unpublished).

[30] L. R. B. Elton (private communication).

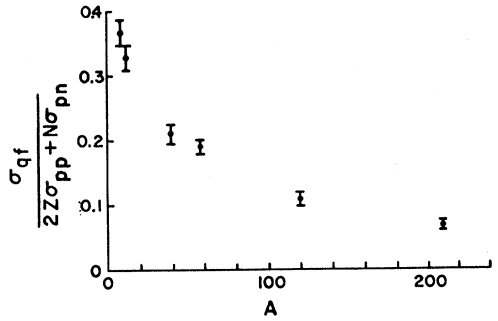

FIG. 7. A plot of the ratios $\sigma_{qf}/(2Z\sigma_{pp}+N\sigma_{pn})$ versus the atomic mass number A, where σ_{qf} is the cross section integrated over the range of angles and over energies from 40 to 60 MeV, N is the neutron number, Z is the atomic number, and σ_{pp} and σ_{pn} are, respectively, the proton-proton and proton-neutron total cross sections.

well depth (rather than on the binding energy as we did for Ca^{40}) and found that to bind the $1s_{1/2}$ state a well depth of 57.45 MeV was necessary, whereas to bind the $1p_{3/2}$ proton a depth of 71.44 MeV was needed. The radius for these two wells was 2.66 F and the rounding parameter was 0.65 F. Be^9 is known to be quite deformed, having a quadrupole moment of 0.03 b. To simulate a deformation we fixed the well depth at 54 MeV and again used ABACUS to find the necessary size nucleus to bind the $1p_{3/2}$ proton, by searching on the radius parameter. We found that it was possible to obtain such a wave function, if for the $p_{3/2}$ state, the radius was increased to 3.15 F. These wave functions made only a very slight difference in the quasifree calculation predictions.

For Ca^{40} the binding energy of the $1s_{1/2}$ state is in fact unknown. Our calculated value is about the same as that deduced from an extrapolation of the recent (e,ep) experiments on aluminum and sulfur.[31] It is believed that the energy dependence of the well depths given in Table II reflects to some degree the correct nonlocality and energy dependence of the optical-model potential which would be given by a detailed Hartree-Fock calculation.

One further simplification made in the present calculations is the lack of differentiation between target neutrons and protons either with respect to the assumed nucleon-nucleon differential cross-sections or single particle binding energies. Finally, to relate the momenta in Eq. (2) to the incident and observed energies we have used a nonrelativistic transformation. The difference between relativistic and nonrelativistic two-body kinematics is less than 3 MeV over the angular range.

Figures 8 and 9 show the prediction of these calculations for the peak position as a function of angle. These figures are analogous to Fig. 6 except that the experimental points are those for the particular element rather than those corresponding to the average over all the target elements. As can be seen, the results for Ca^{40} agree to within about 3 MeV out to 60° but then begin to deviate quite seriously. For Be^9 the shape of the curve for the predicted peak energy as a function of angle is very similar to the experimental shape but is shifted down by about 5 MeV at 10° to a shift at 80° of about 20 MeV. It should be pointed out that in neither of these calculations has any recoil effect been taken into account.

Figures 10 and 11 show the observed and predicted spectra at the indicated angles for Ca^{40} and Be^9. For Ca^{40} the shape of the spectra generally agree very well with the predicted ones. At the peak energies, however, the calculation predicts cross sections which are about a factor of three higher than the experimental values. This factor is slightly angle-dependent being somewhat greater than 3 at forward angles (3.7 at 20°) and less at large angles (2.7 at 60°). For Be^9 the corresponding discrepancy is 1.7 with less angle dependence.

TABLE II. Parameters of a Saxon-Wood potential for the single-particle states of Ca^{40} as given by Elton *et al.* in Ref. 30. The radius and rounding parameters were kept fixed for all the states at $R=1.30A^{1/3}$F and $a=0.60$F.

State	V_0 (MeV)	$V_{\text{spin orbit}}$ (MeV)	Binding energy (MeV) Calc.	Expt.
$1s_{1/2}$	85.0		62.6	
$1p_{3/2}$	60.0	29.8	31.8	
$1p_{1/2}$	60.0	29.8	24.2	24.5
$1d_{5/2}$	53.0	11.7	14.9	15.1
$2s_{1/2}$	53.0		9.8	10.9
$1d_{3/2}$	53.0	11.7	8.2	8.3

[31] U. Amaldi, Jr., *et al.*, Phys. Rev. Letters 13, 341 (1964).

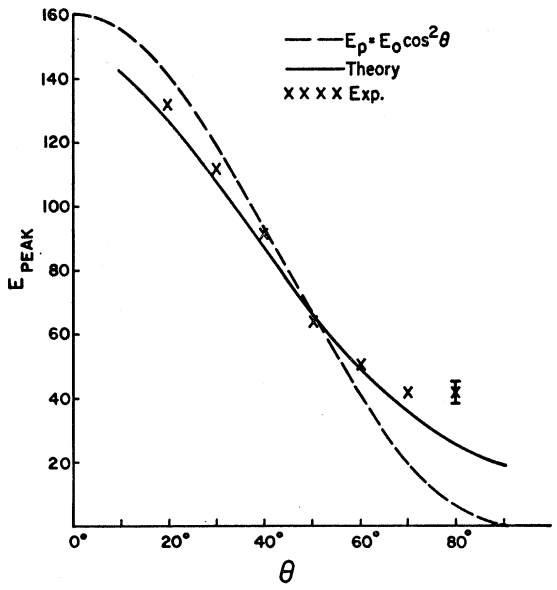

FIG. 8. The energy of the outgoing protons from Ca^{40} at the peak of the quasifree scattering spectrum as a function of the scattering angle. The solid line is the prediction of Eq. (2), the dashed line is free nucleon-nucleon kinematics, and the crosses are the experimental points for Ca^{40}.

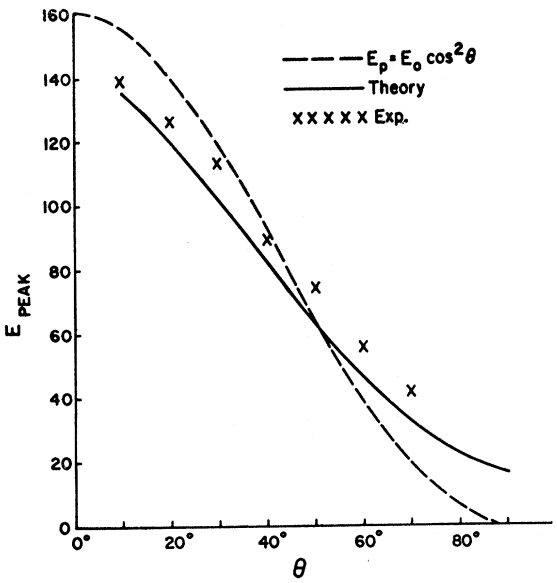

FIG. 9. The energy of the outgoing protons from Be^9 at the peak of the quasifree scattering spectrum as a function of the scattering angle. The solid line is the prediction of Eq. (2), the dashed line is free nucleon-nucleon kinematics, and the crosses are the experimental points for Be^9.

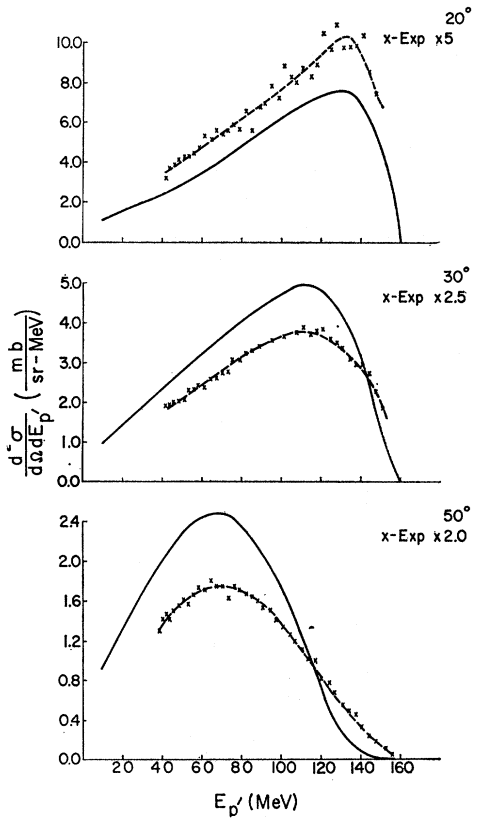

FIG. 10. The spectra predicted by Eq. (2) compared with experiment for 160-MeV incident protons scattered from Ca^{40} at angles of 20°, 30°, and 50°.

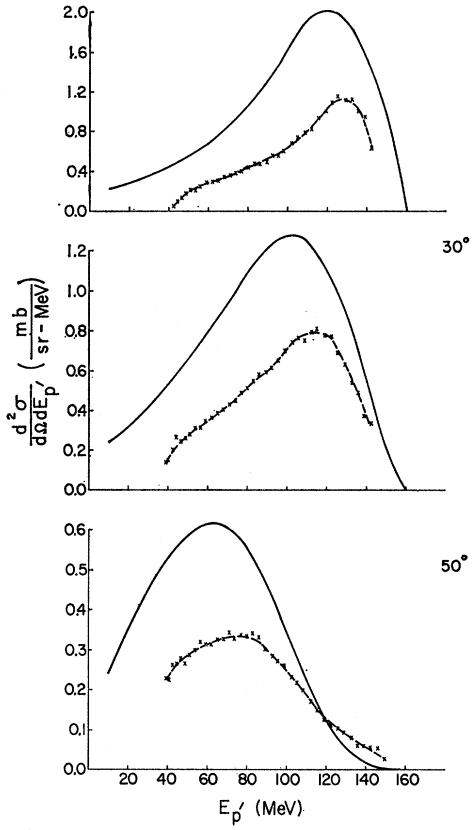

FIG. 11. The spectra predicted by Eq. (2) compared with experiment for 160-MeV incident protons scattered from Be^9 at angles of 20°, 30°, and 50°.

In addition to the type of calculation we have made, Bertini[14] has carried out a Monte Carlo calculation of inelastic proton scattering. This calculation is extremely useful—particularly from the standpoint of estimating the multiple-scattering contributions. The calculation has been described previously in Ref. 14. The calculation essentially follows many incident nucleons through a nucleus composed of A target nucleons allowing the nucleon to make more than one collision and calculates the energy with which the protons come out. The target nucleus is considered to be made up of three regions-each region being described by a Fermi-gas model but with different K_F (Fermi momentum). In this way one gets a density distribution which approximates the density distributions measured in electron scattering. Bertini has used appropriate free nucleon-nucleon cross sections. In addition, a collision taking place in the nucleus must transfer enough momentum to the struck particle to knock it out of the Fermi sea. If not, the collision is ignored and the particle continues unscattered.

Figure 12 shows our experimental spectrum, the result of the Monte Carlo calculation, and the result of looking at just those protons in the Monte Carlo calculation which have undergone only a single collision. The results are at a forward angle (25°–35°) for the calcula-

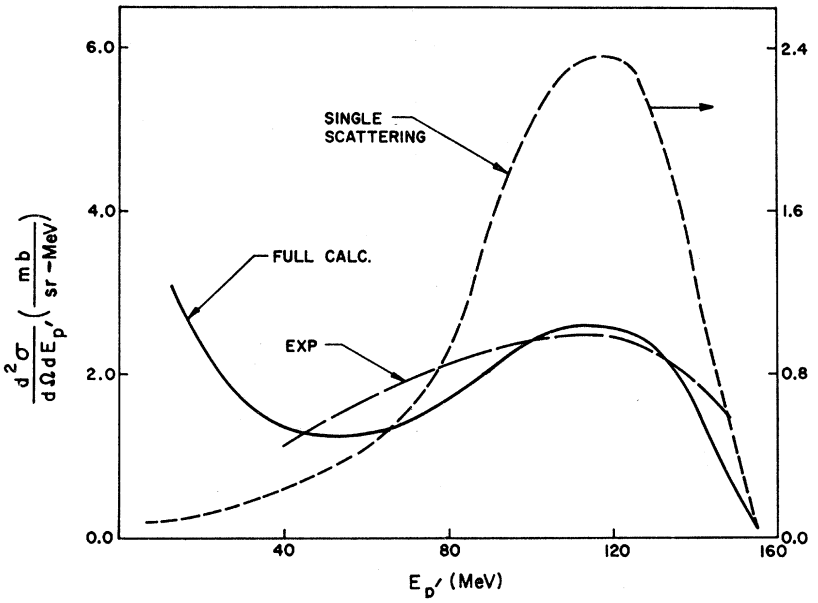

FIG. 12. Monte Carlo calculations for the scattering of 160-MeV protons from Bi^{209} at an average angle of 30°. The curve labeled Full Calc. represents the complete Monte Carlo calculation described in the text. The curve labeled Single scattering represents those particles which escape from the nucleus after a single collision. The experimental results are the data of this experiment. The Monte Carlo results represent a smooth curve drawn through the histogram resulting from tracing 6000 protons through the nucleus and looking at a 10° angular range about 30° and approximately 2- to 8-MeV bin sizes for the energy interval.

tion and are compared with our 30° data for 160-MeV protons incident on Bi^{209}. One sees, in this comparison, rather good agreement between the single-scattering result and our experiment. Also it is clear that when multiple scattering is allowed there is a filling in of the low-energy part of the spectrum, particularly below about 40 MeV, which supports our conjecture that if there is any multiple scattering in our experiments it causes the particle to be shifted below our experimental threshold. Figure 13 shows similar spectra at a larger angle, 60°. Here the multiple-scattering effect is extremely pronounced, but it gives a cross section significantly larger than the Fox and Ramsey (labeled F. R. in Fig. 13) result[31] which is probably a rather typical evaporation spectrum. It should be pointed out that the Monte Carlo calculation of Bertini[14] does not have a specific evaporation contribution. In Fig. 14, the results are given for Be^9 at a fairly large angle. Even in this light nucleus the full Monte Carlo calculation predicts significant multiple scattering.

It should be pointed out that the multiple scattering referred to here is a successive incoherent scattering from the target nucleons, and no possible coherence is taken into account. Nevertheless, using these calculations as a guide we are led to the conclusion that in our experiments we are primarily observing a single-scatter-

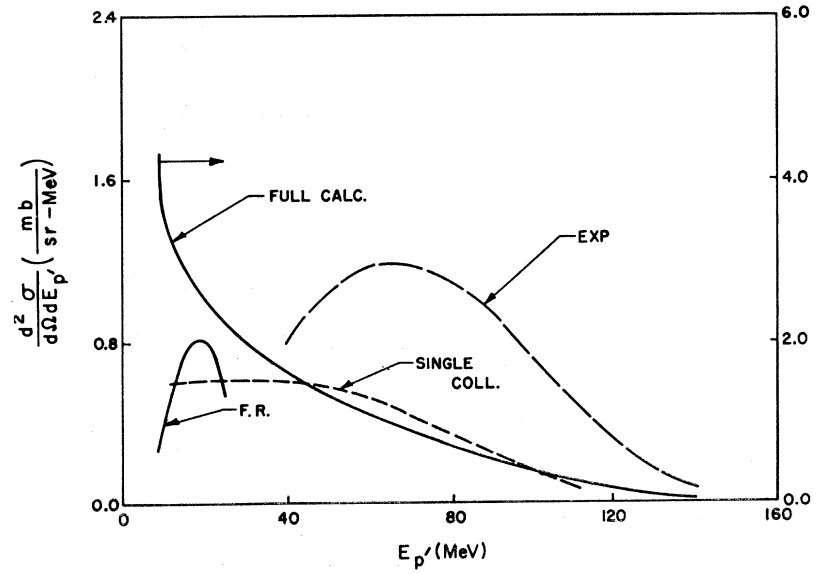

FIG. 13. Monte Carlo calculations for the scattering of 160-MeV protons from Bi^{209} at an average angle of 60°. The curve labeled Full Calc. represents the complete Monte Carlo calculation described in the text. The curve labeled Single Coll. represents those particles which escape from the nucleus after a single collision. The experimental results are the data of this experiment. The Monte Carlo results represent a smooth curve drawn through the histogram resulting from tracing 6000 protons through the nucleus and looking at a 9° angular range about 60° and approximately 2- to 8-MeV bin sizes for the energy interval.

[32] R. Fox and N. F. Ramsey, Phys. Rev. 125, 1609 (1962).

ing process. We have not discussed the sensitivity of the Monte Carlo results to the parameters of the calculation. Only very preliminary study has been made of this because of the large amount of high-speed computer time necessary for each of these calculations. Some indication of the sensitivity of the calculations can be found in Ref. 14.

V. CONCLUSIONS

As pointed our earlier, previous interpretations of similar experiments have been made based upon models which contained only the gross features of the nucleon-momentum distribution. We have, here, used the shell model to derive the momentum distribution so that we automatically build in the correct effects of the single-particle angular momentum and the reflection at the nuclear surface on the bound-state wave functions. Furthermore, our use of experimental binding energies to derive the single-particle wave functions does, to some degree, take into account the residual interactions in a Hartree-Fock sense.[33] The fact that we have utilized a reasonably well-defined nuclear model and obtained a high degree of agreement between experiment and theory in itself lends credence to our calculations and interpretations, and we believe to the interpretations of deviations from the theory.

For Ca^{40} there are two major deviations. The first is the systematic difference for the absolute value of the cross section between the calculated and experimental values at the peak of the spectrum. The fact that our prediction is not as wrong for Be^9 is consistent with the discrepancy arising from an absorptive process. On the other hand, given relatively strong absorption, a question arises as to the validity of the impulse approximation.[12,13] We argue that the absorption is still consistent with the impulse approximation if the essential point of the impulse approximation is that the incident particle collides with individual particles in the nucleus, and that the multiple scattering is primarily an incoherent scattering from different nucleons,[15] as in the sense of the Monte Carlo calculations. Figures 2 through 5 showing similar spectra for all elements, independent of A, provide the strongest evidence for our earlier conjecture that if the absorption processes are strong enough to produce multiple scattering that multiple scattering simply reduces the proton energy below our experimental threshold so that in effect we only observe single scattering. Optical-model parameters[17] which lead to reaction cross sections which are essentially geometric but which have a low (~15 MeV) real part indicate the main effect of the imaginary part is to produce an attenuation but little refraction of the incident or outgoing waves. Therefore the wave functions of the incident and outgoing protons can be treated as plane waves multiplied by a distortion factor which takes into account the absorption. To be able to talk of a momentum distribution, it is necessary that the following proportionality hold:

$$T_{if} \sim \int e^{i\mathbf{q}\cdot\mathbf{r}} \varphi(\mathbf{r}) d\mathbf{r},$$

[33] For example: G. E. Brown, *Unified Theory of Nuclear Models* (John Wiley & Sons, Inc., New York, 1964), Chap. III.

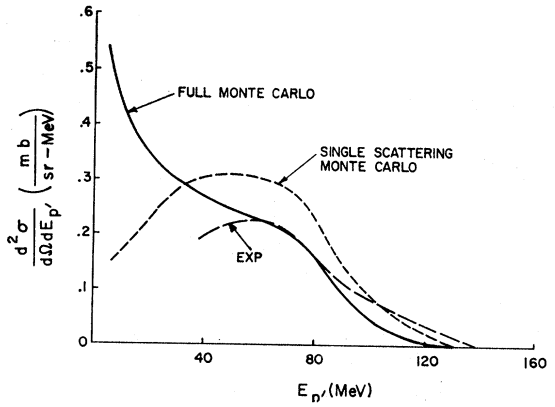

FIG. 14. Monte Carlo calculations for the scattering of 160-MeV protons from Be^9 at an average angle of 60°. The curve labeled Full Monte Carlo represents the complete Monte Carlo calculation described in the text. The curve labeled Single scattering represents those particles which escape from the nucleus after a single collision. The experimental results are the data of this experiment. The Monte Carlo results represent a smooth curve drawn through the histogram resulting from tracing 6000 protons through the nucleus and looking at a 20° angular range about 60° for the full calculation and a 6° angular range about 53° for the single scattering calculation. The bin size varied from 2 to 8 MeV.

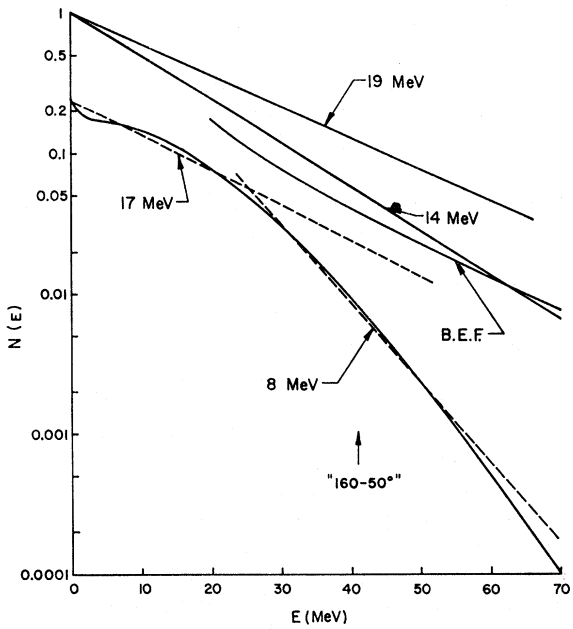

FIG. 15. The momentum distribution derived by Fourier transforming the single particle states in Table 2 and multiplying by $2\times(2j+1)$ to obtain the correct weighting. This is compared with the calculations shown in Fig. 3 of Ref. 33, and Gaussian momentum distributions with characteristic energies of 14 and 19 MeV. The dashed lines show that the single-particle momentum distribution can be approximated by a sum of Gaussians.

where $\varphi(\mathbf{r})$ is the single-particle wave function and $\mathbf{q}$ is the momentum transfer. Such integrals arise in a plane-wave approximation or in the case where it is possible to describe the wave function as a plane wave times an attenuation factor. Therefore the accounting for our observations in terms of single scattering can be consistent with large multiple scattering and the concomitant large total cross sections as well as the optical-model parameters reflecting these phenomena.

The other discrepancy between the calculation and experiment can be seen (particularly from Figs. 10 and 11) to develop at higher outgoing proton energies as the scattering angle is increased. For example, in Ca^{40} at 140 MeV and 50° the measured cross section is about a factor of 3 above the predicted values, rather than the factor of 3 below observed in the vicinity of the peak. Similar effects are observed in the case of Be^{9}. This discrepancy can be described by saying that the single-particle wave functions we have used do not have enough high-momentum components. The average value of K_{MIN} necessary to produce 140-MeV protons at 50° corresponds to momenta in the nucleus of the order of 1.4 F^{1-} (280 MeV/c). As Gottfried[16] has pointed out, the very nature of the processes which give rise to such high momentum components also leads to the breakdown of the type of analysis we are using. In particular, strong short-range two-body correlations would lead to a breakdown of our single-particle model. Brueckner, Eden, and Francis[34] have analyzed the effect of such short-range correlations on experiments similar to ours. They show that the single-particle momentum distribution is in effect modified by the addition of high-momentum components. They indicate that these two-body correlations produce an effective momentum distribution which is similar to a Gaussian with a characteristic energy of the order of 15–20 MeV. Figure 15 shows such momentum distribution and the momentum distribution we derive based on our shell-model approximation for Ca^{40}. We see that our calculation can describe the low-momentum components essentially correctly, but the shell-model momentum distribution drops much too rapidly in the region necessary, for example, to account for the number of 140-MeV protons observed at 50°. In other words, our experiments and calculations indicate that in regions where short-range correlations are expected to be significant there is a marked discrepancy. Whether this discrepancy is a direct manifestation of short-range correlations, the breakdown of the impulse approximation, or "off-the-energy-shell" effects we cannot say definitely in this type of experiment.[16]

There is one possible source of these high momenta beyond those mentioned above, namely the scattering from quasiparticles representing collective states. Insofar as the low-lying (3.73- and 4.48-MeV) strongly collective states of Ca^{40} are concerned, it is interesting to observe their cross-section is much less than twice the integrated cross-section between 10-MeV and 20-MeV excitation. Furthermore, it is known that these states represent at least half the 2^3 pole and 2^5 pole strength observed in elastic alpha-particle scattering.[35] This suggests that the contributions in this energy region are not indicative of residual shell-model interactions. In the language of inelastic electron scattering, the form factor for the excitation of these collective states represents such coherent processes that they become quite small when the momentum transfer is sufficiently large, at 50° this is of the order of $2.4F^{-1}$.

One might also attempt to take into account further corrections to our extreme model by utilizing a quasiparticle description of the target nucleons as has Reiner[36] in the case of inelastic electron scattering. However, the use of experimental binding energies, particularly in the case of the low-lying levels of the shell-model potential, takes into account some of the effects of the other nucleons.[37,38].

While one could improve on our calculation by taking into account the energy and angular dependence of the nucleon-nucleon cross section they are known well enough[26,27] to know that they could not account for the observed effects.[39] We believe that the next phase of the analysis should be to take into account the absorption of the incident and outgoing particles by allowing them to move in complex optical potentials, and insofar as possible build in the correlation effects to this distorted-wave calculations following Ref. 33.

ACKNOWLEDGMENTS

The authors would like to thank A. Koehler and Dr. B. Gottschalk for considerable help during the execution of these experiments. They would like to thank Dr. H. Bertini for supplying them with the appropriate Monte Carlo calculations. We would like to acknowledge the use of Dr. J. Ball's program for the scattering-out correction. A particular debt of gratitude is due M. Joseph and R. Kroll for considerable assistance in the calculations reported here.

[34] K. A. Brueckner, R. J. Eden, and N. C. Francis, Phys. Rev. **98**, 1445 (1955).

[35] R. W. Bauer *et al.*, Phys. Letters **14**, 129 (1965).

[36] A. S. Reiner, Phys. Rev. **138**, B389 (1965).

[37] K. A. Brueckner, in *Proceedings of the Rutherford Jubilee International Conference, Manchester, 1961* (Heywood and Company, Ltd., London, 1961), pp. 32, 386.

[38] K. A. Brueckner, R. J. Eden, and N. C. Francis, Phys. Rev. **100**, 891 (1955).

[39] Riley (Ref. 25) gives $d^2/d\Omega dE=(1.9+230/E+4850/E^2)\times(1+0.1\cos^2\theta)$ as an empirical formula for p-p scattering accurate to about 10% in the range 100–800 MeV.